

## Supporting Information

### Oligomeric Semiconductors Enable High Efficiency Open Air Processed Organic Solar Cells by Modulating Pre-aggregation and Crystallization Kinetics

Hao Xia,<sup>a,b</sup> Ying Zhang,<sup>\*b</sup> Kuan Liu,<sup>b</sup> Wanyuan Deng,<sup>c</sup> Mengbing Zhu,<sup>a</sup> Hua Tan,<sup>a</sup> Patrick W K Fong,<sup>b</sup> Heng Liu,<sup>d</sup> Xinxin Xia,<sup>d</sup> Miao Zhang,<sup>e</sup> Top Archie Dela Peña,<sup>figh</sup> Ruijie Ma,<sup>b</sup> Mingjie Li,<sup>g</sup> Jiaying Wu,<sup>f</sup> Yongwen Lang,<sup>b</sup> Jiehao Fu,<sup>b</sup> Wai-Yeung Wong,<sup>c</sup> Xinhui Lu,<sup>d</sup> Weiguo Zhu,<sup>\*a</sup> Gang Li<sup>\*b</sup>

*<sup>a</sup>School of Materials Science and Engineering, Jiangsu Engineering Laboratory of Light-Electricity-Heat Energy-Converting Materials and Applications, Jiangsu Collaborative Innovation Center of Photovoltaic Science and Engineering, National Experimental Demonstration Center for Materials Science and Engineering, Changzhou University, Changzhou 213164, China.*

*<sup>b</sup>Department of Electronic and Information Engineering, The Hong Kong Polytechnic University, Hung Hum Kowloon, Hong Kong 999077, China*

*<sup>c</sup>State Key Laboratory of Luminescent Materials and Devices, Institute of Polymer Optoelectronic Materials and Devices, South China University of Technology, Guangzhou 510640, China*

*<sup>d</sup>Department of Physics, The Chinese University of Hong Kong, New Territories, Hong Kong 999077, China*

*<sup>e</sup>Department of Applied Biology and Chemical Technology, The Hong Kong Polytechnic University, Hung Hum Kowloon, Hong Kong 999077, China*

*<sup>f</sup>The Hong Kong University of Science and Technology, Function Hub, Advanced Materials Thrust, Nansha 511400, Guangzhou, P. R. China*

*<sup>g</sup>The Hong Kong University of Science and Technology, School of Science, Department of Chemistry, Kowloon, Hong Kong 999077, P.R. China*

*<sup>h</sup>The Hong Kong Polytechnic University, Faculty of Science, Department of Applied Physics, Kowloon, Hong Kong 999077, P.R. China;*

Email addresses:

Yingeva.zhang@polyu.edu.hk

zhuwg18@126.com(W.Z.)

gang.w.li@polyu.edu.hk (G.L.)

## **Table of Contents**

- 1. Measurement and characterization.**
- 2. Device fabrication method.**
- 3. Material synthesis and characterization.**
- 4. The relevant test results of UV, DFT,  $J$ - $V$ , PL, SCLC, GIWAXS, In Situ UV, AFM, Contact Angle, Stability.**
- 5.  $^1\text{H}$ -NMR ,  $^{13}\text{C}$ -NMR and MALDI-TOF.**

## 1. Measurement and characterization

$^1\text{H}$  NMR and  $^{13}\text{C}$  NMR spectra were taken on a Bruker AV 400 Spectrometer. Mass spectra were measured on a Bruker Daltonics BIFLEX III matrix assisted laser desorption/ionization time-of-flight (MALDI-TOF) analyzer. UV-vis spectra were obtained with the Cary 4000 UV-Vis spectrophotometer. Cyclic voltammetry (CV) experiments were performed with a LK98B II microcomputer based electrochemic analyzer in dichloromethane solutions. All CV measurements were carried out at room temperature with a conventional three-electrode configuration employing a Pt disk, a Pt plate and an Ag/AgCl electrode as working electrode, counter electrode and reference electrode, respectively. Tetrabutylammonium phosphorus hexafluoride ( $\text{Bu}_4\text{NPF}_6$ , 0.1 M) in acetonitrile was used as the supporting electrolyte, and the scan rate was  $100 \text{ mVs}^{-1}$ . For calibration, the redox potential of ferrocene/ferrocenium ( $\text{Fc}/\text{Fc}^+$ ) was measured under the same conditions. Atomic force microscopy (AFM) was performed using a multimode 8 atomic force microscope in tapping mode. GIWAXS measurements were carried out with a Xeuss 2.0 SAXS/WAXS laboratory beamline using a Cu X-ray source (8.05 keV, 1.54 Å) and Pilatus 3R 300 K detector. The incidence angle is  $0.2^\circ$ .

The current density-voltage ( $J$ - $V$ ) curves of photovoltaic devices were obtained by a Keithley 2400 source-measure unit. The photocurrent was measured under illumination simulated  $100 \text{ mW cm}^{-2}$  AM 1.5G irradiation using an Oriel 96000 solar simulator, calibrated with a standard Si solar cell. The average PCE was obtained using 15 devices under the same conditions. External quantum efficiency (EQE) values of devices were

measured using Stanford Research Systems QE-R3-011. The thickness of the active layers in the photovoltaic devices was measured on a Veeco Dektak 150 profilometer. SCLC mobility was measured using a diode configuration of Glass/ITO/PEDOT:PSS/active layer/MoO<sub>3</sub>/Ag for hole and Glass/ITO/ZnO/Active Layer/PFN-Br/Ag for electron by taking the dark current density in the range of 0-4 V and fitting the results to a space charge limited form, where SCLC is described by:

$$J = \frac{9\varepsilon_0\varepsilon_r\mu_0V^2}{8L^3}$$

Where  $J$  is the current density,  $L$  is the film thickness of the active layer,  $\mu_0$  is the hole or electron mobility,  $\varepsilon_r$  is the relative dielectric constant of the transport medium,  $\varepsilon_0$  is the permittivity of free space ( $8.85 \times 10^{-12}$  F m<sup>-1</sup>),  $V$  ( $= V_{\text{appl}} - V_{\text{bi}}$ ) is the internal voltage in the device, where  $V_{\text{appl}}$  is the applied voltage to the device and  $V_{\text{bi}}$  is the built-in voltage due to the relative work function difference of the two electrodes.

## 2. Device fabrication method

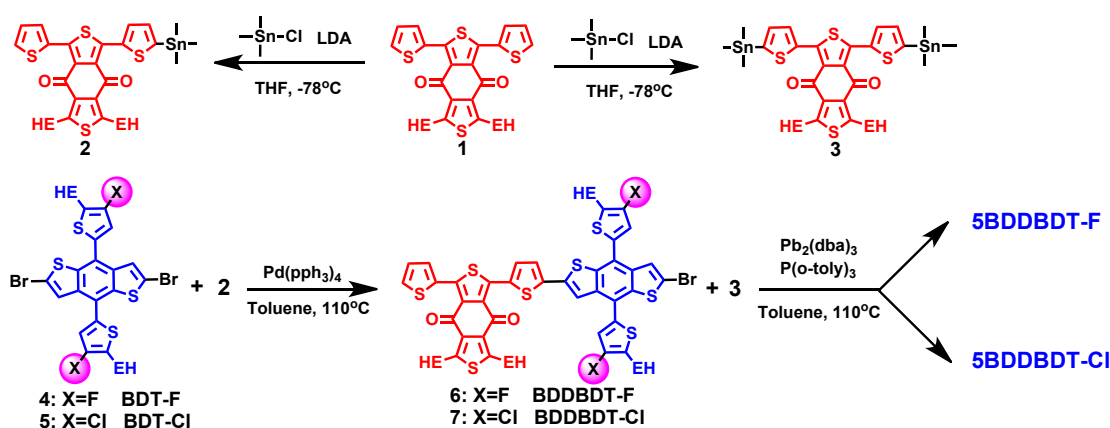
Spin coating device: the device structure was Glass/ITO/PEDOT:PSS/active layer/PFN-Br/Ag. A glass substrate with a pre-patterned ITO (sheet resistance = 15  $\Omega\text{sq}^{-1}$ ) was ultrasonicated subsequently in detergent, deionized water, acetone, and isopropanol. After the plates were dried by high-pressure air flow, the substrates were cleaned by UV-ozone treatment for 20 min. PEDOT:PSS (4083) was spin-coated on the substrates at 4000 rpm for 30 s in dry air, which were then baked on a hot plate at 150 °C for about 15 min. After cooling to room temperature, the substrates were sent to an argon-filled glove box. A blend film of Donor:Acceptor (1:1.2 w/w,) was prepared by spin-coating its mixed solution in O-xylene/1,8-diiodoctane (donor concentration:

10, 0.5% DIO) at 3000 rpm for 60 s, then thermal annealing at 100 °C 10 min or not. After cooled to room temperature, spin-coating a thin layer (5 nm) of PFN-Br on the active layer, and Ag cathode (100 nm) were deposited by using thermal evaporation in a high vacuum chamber ( $\sim 10^{-5}$  mbar). was measured using a Dektak 6 M surface profilometer. The device area was exactly fixed at 4.0 mm<sup>2</sup>. The *J-V* characterization of the devices was carried out on a computer-controlled Keithley 2400 Source Measurement system with a solar simulator (XES-70S1, SAN EI Co., Ltd.) was used as the light source. The light intensity was monitored by using a standard Si solar cell (KONICA MINOLTA, INC.).

Blade coating device: all processes are the same as spin coating devices, except the fabrication of the active layer. the active layer solutions were prepared by o-xylene solutions (D:A = 1:1.2 w/w, 10 mg mL<sup>-1</sup> donor concentration, for binary and ternary blends), stirring for 3 h at 55°C to ensure the donor and acceptor dissolve completely. The blade speed was about 20 mm s<sup>-1</sup>. The gap between the film applicator and substrate was about 100-150 μm. When coating the active layer, the ITO-based substrate was maintained at 60 °C. Then, the active layer solution was dripped on the substrate and swiped linearly to form a film. A laminar nitrogen knife releases the nitrogen gas to accelerate the drying of the film. Then, the substrate was moved to the glove box, PFN-Br was spin-coated on the active layer, and silver cathodes were deposited using thermal evaporation.

### **3. Material Synthesis and Characterization**

Compound 1, 4 and 5 were purchased from Nanjing Zhiyan Technology Co., Ltd. Other organic reagents were purchased from chemical reagent suppliers and used without further purification. Toluene and tetrahydrofuran were distilled according to common methods. Column chromatography was carried out with Merck silica gel (200 – 300 mesh).



**Scheme 1.** Synthetic routes of 5BDDBDT-F and 5BDDBDT-Cl.

### Synthesis of compound 6

In a 100 mL two-neck round-bottom flask, a mixture of compound 4 (0.50 g, 0.65 mmol), compound 2 (0.33 g, 0.43 mmol), and Pd(pph<sub>3</sub>)<sub>4</sub> (19.60 mg, 0.02 mmol) in toluene was degassed under the N<sub>2</sub> atmosphere and stirred at refluxing temperature for 12 h. After cooled to room temperature, the mixture was poured into water (150 mL), and extracted with CH<sub>2</sub>Cl<sub>2</sub>(30 mL×3). The organic phases were combined and dried over with anhydrous MgSO<sub>4</sub>. The solvents were removed under reduced pressure. The red residue was purified by silica gel chromatography, eluting with PE-CH<sub>2</sub>Cl<sub>2</sub> (5:1) to give a red solid (0.26 g, 46 %). <sup>1</sup>H NMR (500 MHz, CDCl<sub>3</sub>) δ 7.74 (d, *J* = 4.8 Hz, 1H), 7.70 (d, *J* = 3.4 Hz, 2H), 7.58 (s, 1H), 7.50 (d, *J* = 5.1 Hz, 1H), 7.27 (d, *J* = 4.0 Hz, 1H),

7.13 (d,  $J = 1.4$  Hz, 2H), 7.11 (dd,  $J = 5.1, 3.8$  Hz, 1H), 3.39-3.24 (m, 4H), 2.80 (d,  $J = 6.7$  Hz, 4H), 1.76-1.74 (m, 2H), 1.71 – 1.64 (m, 2H), 1.44 – 1.25 (m, 32H), 0.97-0.86 (m, 24H).  $^{13}\text{C}$  NMR (126 MHz,  $\text{CDCl}_3$ )  $\delta$  177.64, 177.45, 155.43, 153.65, 153.55, 153.40, 142.45, 141.66, 140.28, 140.22, 138.65, 138.26, 136.87, 136.12, 134.05, 133.39, 133.28, 132.99, 132.88, 132.57, 132.52, 131.42, 130.69, 129.55, 127.20, 125.82, 125.61, 122.78, 122.73, 122.64, 122.59, 122.31, 119.07, 118.22, 118.16, 118.00, 117.94, 117.23, 41.24, 41.20, 40.85, 33.63, 32.81, 32.76, 32.54, 32.50, 29.75, 29.20, 28.86, 28.81, 26.94, 26.17, 26.00, 25.79, 23.06, 23.00, 14.21, 14.18, 11.00, 10.90, 10.87.

### Synthesis of compound 7

The synthesis method of compound 7 can refer to that of compound 6. Compound 5 (0.50 g, 0.62 mmol), compound 2 (0.32 g, 0.41 mmol), and  $\text{Pd}(\text{pPh}_3)_4$  (18.77 mg, 0.02 mmol) are the raw materials, and give red solid compound 7 (0.26 g, 48 %).  $^1\text{H}$  NMR (400 MHz,  $\text{CDCl}_3$ )  $\delta$  7.73 (s, 2H), 7.70 (d,  $J = 4.0$  Hz, 1H), 7.67 (s, 1H), 7.49 (d,  $J = 5.0$  Hz, 1H), 7.24 (dd,  $J = 20.4, 3.9$  Hz, 3H), 7.11 (dd,  $J = 5.0, 3.9$  Hz, 1H), 3.41 – 3.22 (m, 4H), 2.85 (d,  $J = 6.7$  Hz, 4H), 1.81 – 1.68 (m, 4H), 1.51 – 1.19 (m, 44H), 0.93 (dt,  $J = 23.9, 9.8$  Hz, 28H), 0.00 (s, 1H).  $^{13}\text{C}$  NMR (101 MHz,  $\text{CDCl}_3$ )  $\delta$  177.71, 177.51, 153.78, 153.63, 140.28, 138.80, 138.59, 137.43, 135.14, 133.29, 133.02, 132.92, 131.47, 130.72, 129.58, 128.17, 127.25, 123.09, 122.98, 121.89, 121.47, 119.01, 41.31, 41.24, 40.92, 40.86, 33.66, 32.83, 32.77, 32.56, 32.50, 32.15, 29.75, 28.83, 26.18, 26.02, 25.83, 23.07, 23.01, 14.23, 14.19, 11.04, 10.91.

### Synthesis of compound 5BDDBDT-F

In a 50 mL two-neck round-bottom flask, a mixture of compound 6 (0.36 g, 0.028 mmol), compound 3 (0.1 g, 0.11 mmol) and Pd<sub>2</sub>(dba)<sub>3</sub> (5.04 mg, 0.0055 mmol), tri(o-tolyl)phosphine (6.70 mg, 0.022 mmol) in toluene was degassed toluene and stirred at refluxing temperature for 12 h under the N<sub>2</sub> atmosphere. After cooled to room temperature, the mixture was poured into water (150 mL), and extracted with CH<sub>2</sub>Cl<sub>2</sub>(30 mL×3). The organic phases were combined and then dried over with anhydrous MgSO<sub>4</sub>. The solvents were removed under reduced pressure. The purple-black residue was purified by silica gel chromatography eluting with PE-CH<sub>2</sub>Cl<sub>2</sub> (1:1) to give purple-black solid (0.22 g, 65 %). <sup>1</sup>H NMR (400 MHz, CDCl<sub>3</sub>) δ 7.60 (s, 2H), 7.48 (s, 2H), 7.36 (s, 6H), 7.28 (s, 2H), 7.21 (s, 4H), 6.95 (s, 2H), 6.86 (d, *J* = 12.1 Hz, 4H), 3.42 (s, 4H), 3.13 (d, *J* = 41.9 Hz, 8H), 2.90 (s, 8H), 1.77-1.71 (m, 10H), 1.47-1.25 (m, 80H), 1.08-0.88 (m, 60H). <sup>13</sup>C NMR (101 MHz, CDCl<sub>3</sub>) δ 177.17, 153.15, 152.74, 141.93, 141.77, 140.80, 140.23, 138.27, 137.30, 136.77, 133.98, 133.62, 133.43, 132.88, 132.81, 132.13, 131.24, 130.44, 129.36, 126.81, 124.86, 122.33, 122.04, 121.85, 118.65, 41.29, 41.04, 40.71, 33.51, 32.95, 32.76, 32.62, 29.72, 29.46, 28.89, 28.75, 26.37, 25.97, 25.74, 23.16, 23.07, 14.28, 14.18, 11.34, 11.18, 10.85, 10.82. MALDI-MS (*m/z*) of C<sub>170</sub>H<sub>192</sub>F<sub>4</sub>O<sub>6</sub>S<sub>20</sub> for [M<sup>+</sup>]: calcd. 3048.594; found, 3047.911.

### **Synthesis of compound 5BDDBDT-Cl**

The synthesis method of compound 5BDDBDT-Cl can refer to that of compound 5BDDBDT-F. Compound 7 (0.37 g, 0.028 mmol), compound 3 (0.1 g, 0.11 mmol) and Pd<sub>2</sub>(dba)<sub>3</sub> (5.04 mg, 0.0055 mmol), tri(o-tolyl) phosphine (6.70 mg, 0.022 mmol) are

the raw materials, and give purple-black solid (0.34 g, 68%).  $^1\text{H}$  NMR (400 MHz,  $\text{CDCl}_3$ )  $\delta$  7.72 (d,  $J = 3.4$  Hz, 2H), 7.69 (d,  $J = 3.9$  Hz, 2H), 7.57 (s, 6H), 7.47 (d,  $J = 5.1$  Hz, 2H), 7.33 (d,  $J = 2.0$  Hz, 4H), 7.14-7.12 (m, 4H), 7.09-7.07 (m, 2H), 3.45-3.40 (m, 4H), 3.27-3.27 (m, 8H), 2.96 (d,  $J = 6.7$  Hz, 8H), 1.87-1.79 (m, 10H), 1.54-1.32 (m, 80H), 1.07-0.92 (m, 60H).  $^{13}\text{C}$  NMR (101 MHz,  $\text{CDCl}_3$ )  $\delta$  177.32, 153.16, 142.08, 141.80, 141.74, 140.68, 140.24, 138.66, 138.25, 137.77, 137.69, 137.02, 135.55, 133.81, 133.73, 133.36, 132.86, 132.34, 132.09, 131.82, 131.37, 130.59, 129.47, 128.06, 127.01, 125.34, 123.00, 122.96, 122.25, 118.93, 41.29, 41.20, 41.11, 40.70, 33.57, 32.89, 32.74, 32.58, 32.33, 28.84, 26.27, 25.97, 25.81, 23.13, 23.04, 23.02, 14.26, 14.18, 11.27, 11.14, 10.88. MALDI-MS ( $m/z$ ) of  $\text{C}_{170}\text{H}_{192}\text{Cl}_4\text{O}_6\text{S}_{20}$  for  $[\text{M}^+]$ : calcd. 3114.400; found, 3113.789.

#### 4. The Relevant Test Results of UV, DFT, $J$ - $V$ , PL, SCLC, GIWAXS, Contact Angle and Energy Loss

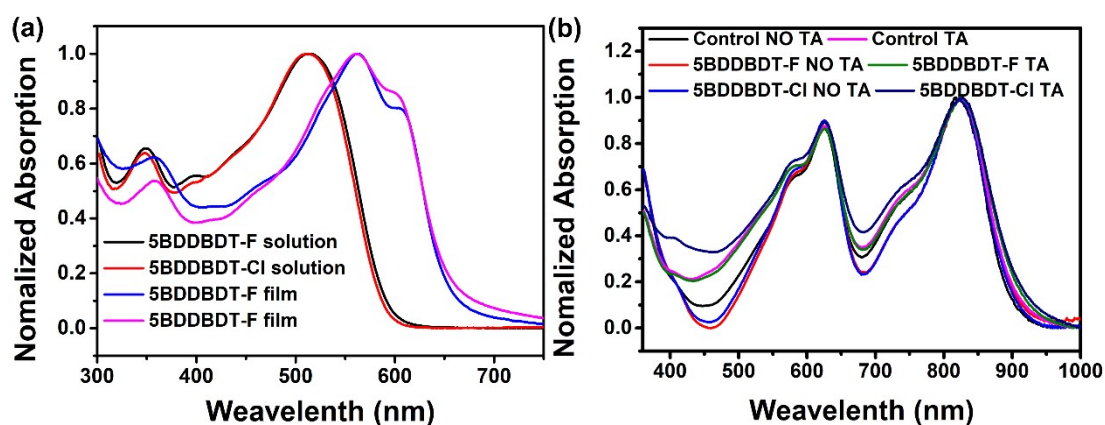
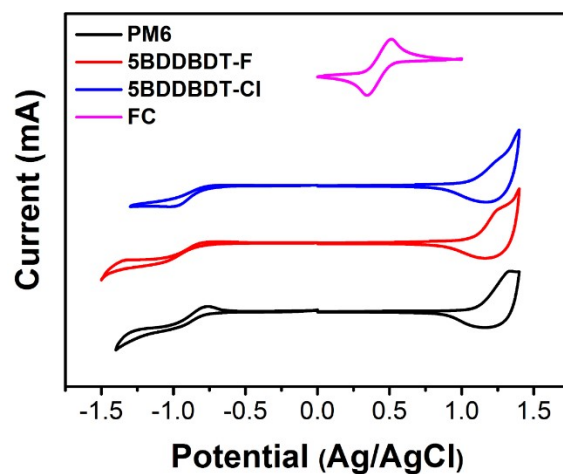
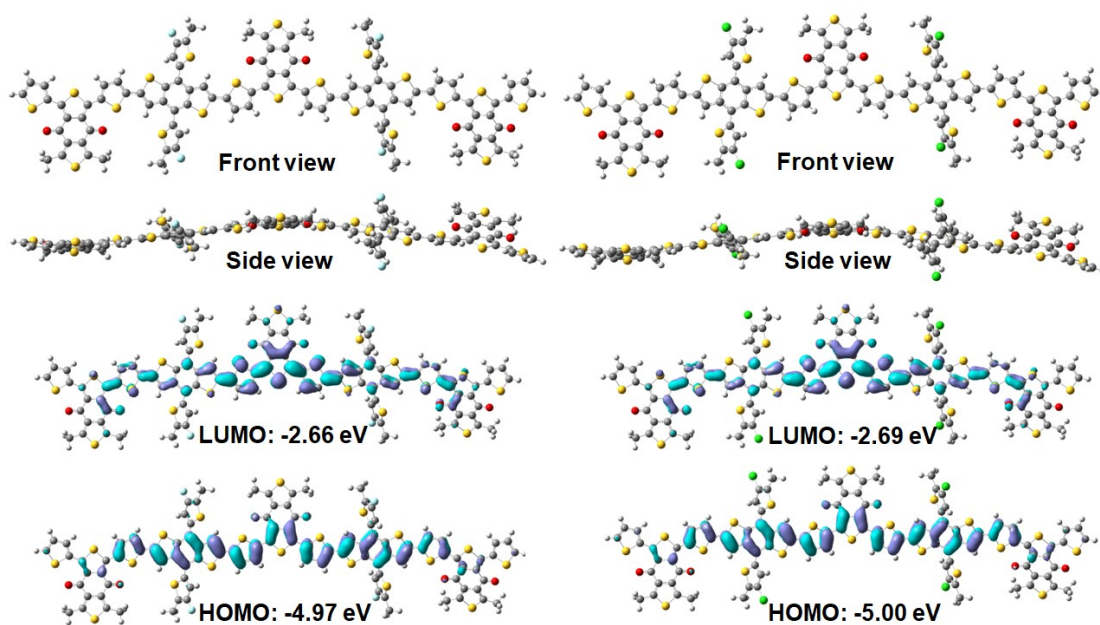


Figure S1 UV-vis absorption spectra in dilute *o*-XY solution and neat films by normalized treatment.



**Figure S2** CV curves of PM6, 5BDDBDT-F and 5BDDBDT-Cl .



**Figure S3** Optimized geometries views parallel to the molecular planes and HOMO and LUMO orbitals calculated for 5BDDBDT-F and 5BDDBDT-Cl using Gaussian at the B3LYP/6-31G\* level

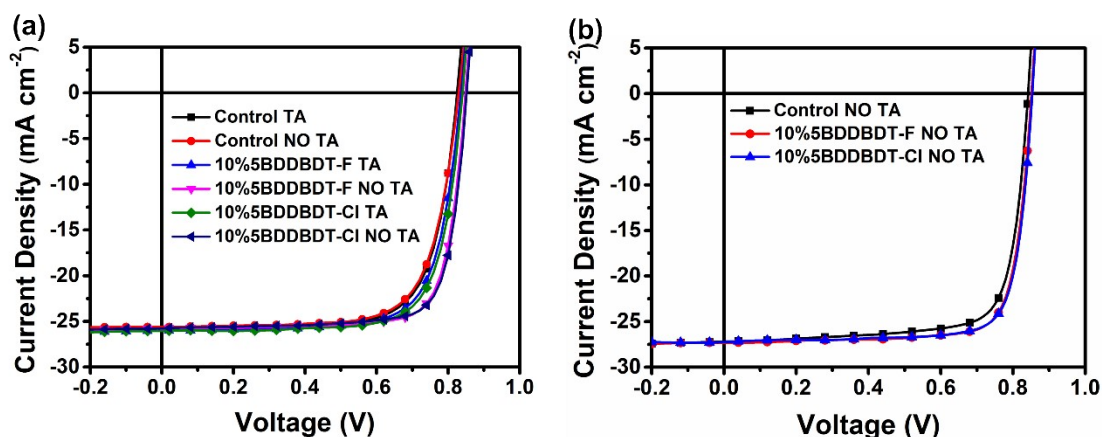


**Figure S4** (a)  $J$ - $V$  curves of control, 10%5BDDDBDT-F and 10%5BDDDBDT-CI small area ternary blade coating devices based on PM6:oligomer:BTP-BO4Cl system at an optimal processing condition under a simulated AM 1.5 G irradiation ( $100 \text{ mW cm}^{-2}$ ). (b)  $J$ - $V$  curves of control, 10%5BDDDBDT-F and 10%5BDDDBDT-CI small area ternary spin coating devices based on PM6:oligomer:BTP-eC9 system using CB as solvent at an optimal processing condition under a simulated AM 1.5 G irradiation ( $100 \text{ mW cm}^{-2}$ ).

**Table S1.** The photovoltaic parameters of the binary and ternary devices based on PM6:oligomer:BTP-BO4Cl system.

Third ratio	component	Coating method	Area ( $\text{cm}^2$ )	Treatment	$V_{OC}$ (V)	$J_{SC}^a$ ( $\text{mA cm}^{-2}$ )	$J_{SC}^{EQE}$ ( $\text{mA cm}^{-2}$ )	FF (%)	$PCE_{max}^b$ (%)
Control		Blade coating	0.04	TA	0.825	25.93	25.08	72.76	15.57
		Blade coating		NO TA	0.829	25.60	24.95	72.33	15.35
10%5BDDDBDT-F		Blade coating	0.04	TA	0.836	26.02	25.23	73.62	16.01
		Blade coating		NO TA	0.848	25.77	25.16	78.36	17.13
10%5BDDDBDT-CI		Blade coating	0.04	TA	0.840	26.04	25.18	74.13	16.21
		Blade coating		NO TA	0.851	25.76	24.89	78.25	17.15

<sup>a</sup> $J_{SC}$  measured from devices. <sup>b</sup>PCE Obtained from 10 devices, with 0.4% DIO additive.

**Table S2.**

Time	Donor	Acceptor	Green solvent	$V_{OC}$ (V)	$J_{SC}$ ( $\text{mA cm}^{-2}$ )	FF (%)	$PCE_{max}$ (%)	Ref.
2020	PM6	TB-4Cl	NO	0.848	22.99	75.20	14.67	[1]
2019	PBDB-T	m-INPOIC :PC <sub>71</sub> BM	NO	0.857	21.3	71.6	14.00	[2]
2020	PM6	Y6	NO	0.852	25.33	74.39	16.06	[3]
2020	PM6	Y18	NO	0.87	23.86	63.6	13.38	[4]
2021	PM6	DCB-4F :PC <sub>71</sub> BM	NO	1.00	16.79	66.53	11.17	[5]
2020	PTB7-Th	PC <sub>71</sub> BM	NO	0.80	17.47	71.27	10.53	[6]
2021	PM6	Y6	NO	0.84	23.92	72.9	14.66	[7]
2020	PM6	Y6Se	NO	0.839	27.98	75.3	17.7	[8]
2021	PM6	NFA1:NFA2	NO	0.896	24.86	74.8	16.68	[9]
2020	PTB7-Th	F10IC2	YES	0.769	23.1	65.8	11.7	[10]
2022	PM6	BTP-eC9	YES	0.85	26.2	78.9	17.6	[11]
2021	PM6	Y6:20%BTO :PC <sub>71</sub> BM	YES	0.85	27.12	75.75	17.41	[12]
2020	PM6	Y11	NO	0.897	24.30	63.00	13.80	[13]

2022	PM6	Y6	NO	0.84	24.74	77.25	16.07	[14]
2022	PM6	Y-FIC- $\gamma$ e	NO	0.877	25.86	71.85	16.39	[15]
2020	PM6	C6	NO	0.84	23.82	72.68	14.54	[16]
2022	PM6:PM7	Y6:20% BTO	YES	0.86	27.19	76.05	17.78	[17]
2022	PM6	A1	YES	0.84	26.5	74.5	16.8	[18]
2023	PM6	m-BzY	YES	0.888	24.4	74.5	16.1	[19]
2022	PM6	BTP-eC9	NO	0.89	26.5	72.7	17.4	[20]
2019	PM6	POIT-IC4F	NO	0.91	20.9	72.6	13.8	[21]
2023	PM6:5BDDBDT-F	BTP-eC9	<b>YES</b>	0.850	27.25	78.12	18.09	<b>This work</b>
2023	PM6:5BDDBDT-Cl	BTP-eC9	<b>YES</b>	0.853	27.11	78.49	18.15	<b>This work</b>

**Table S3.**

Time	Donor	Acceptor	Green solvent	In open air	TA treatment	V <sub>oc</sub> (V)	J <sub>sc</sub> (mA cm <sup>-2</sup> )	FF (%)	PCE (%)	Ref.
2019	PM6	Y6:N2200	YES	NO	YES	0.83	26.2	69	15.1	[22]
2019	PBDB-T-2F	IT-4F	NO	NO	YES	0.86	21.1	72	13.2	[23]
2020	PM6	ITIC-4F: ICBA	NO	NO	YES	0.871	20.64	73.30	13.7	[24]
2021	PM6	BTP-eC9	NO	NO	YES	0.83	24.9	73	15.1	[25]
2021	PM6	Y6	YES	NO	YES	0.836	24.48	67.87	13.87	[26]
2022	PM6	BTP-eC9	YES	NO	YES	0.820	25.37	71.18	14.82	[27]
2018	PBTA-TF	IT-M	YES	YES	NO	0.95	17.13	65	10.6	[28]
2019	PM6	IT-4F	YES	YES	NO	0.84	19.5	65	11.4	[29]
2019	T1	IT-4F	NO	NO	YES	0.861	21.8	70	13.1	[30]
2022	PBDB-T	PYSe-TCl20: PTCl <sub>o</sub> -Y	NO	YES	YES	0.908	23.3	68.1	13.81	[30]
2019	T1	BTP-4F-12	YES	NO	YES	0.85	24.2	70	14.4	[32]
2022	PM6	Y6	NO	YES	NO	0.83	25.52	65.96	13.94	[33]
2020	PBDB-T-2F	Y6	NO	NO	YES	0.836	25.46	70.7	15.08	[34]
2023	PM6	L8-BO	NO	NO	YES	0.90	24.8	74.3	16.6	[35]
2022	PTQ10	Y6-BO	NO	NO	YES	0.85	25.62	59.55	13.48	[36]
2021	PM6	PYF-T-o	NO	YES	YES	0.909	22.6	63.4	13.0	[37]
2022	PM6	N3: P(NDI2OD-T2)	NO	YES	NO	0.854	24.74	66.83	14.12	[38]
2022	PM6	BTP-eC9: PC <sub>71</sub> BM	NO	NO	YES	0.832	27.06	70.2	15.82	[39]
2022	PM6	AITC:BTP-eC9	NO	YES	YES	0.85	25.9	75.7	16.7	[40]
2023	PM6	BTP-eC9	NO	NO	YES	0.834	28.1	65.6	15.4	[41]
2023	PM6:5BDDBDT-F	BTP-eC9	<b>YES</b>	<b>YES</b>	<b>NO</b>	0.850	27.54	73.09	17.11	<b>This work</b>
2023	PM6:5BDDBDT-Cl	BTP-eC9	<b>YES</b>	<b>YES</b>	<b>NO</b>	0.853	27.37	73.08	17.06	<b>This work</b>

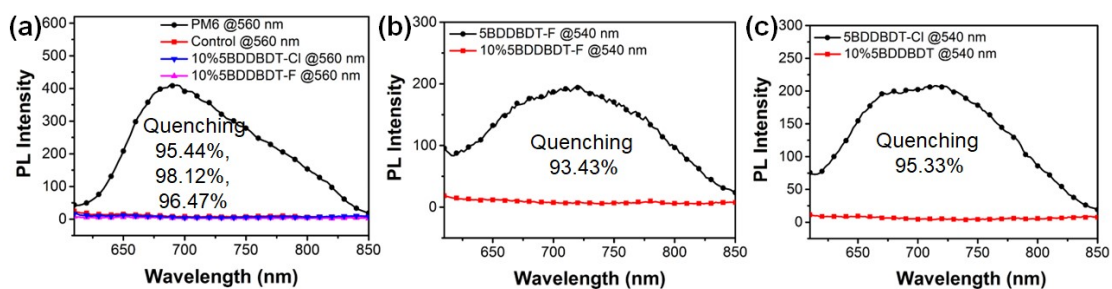


**Figure S5.** Photoluminescent spectra of the pure and blend films excited at (a) 560 nm, (b) 540 nm, and (c) 540 nm.

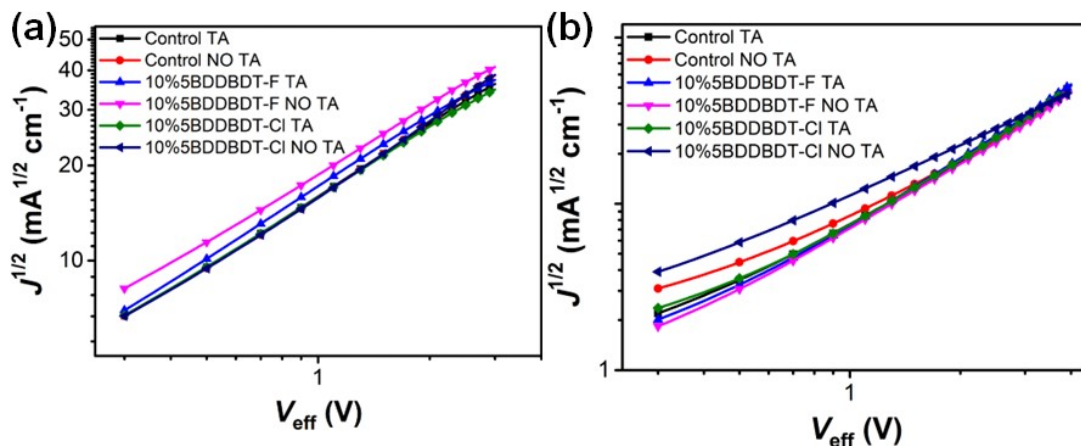


**Figure S6.** (a)  $J^{1/2}$ - $V$  characteristics of the hole-only devices; (b)  $J^{1/2}$ - $V$  characteristics of the electron-only devices.

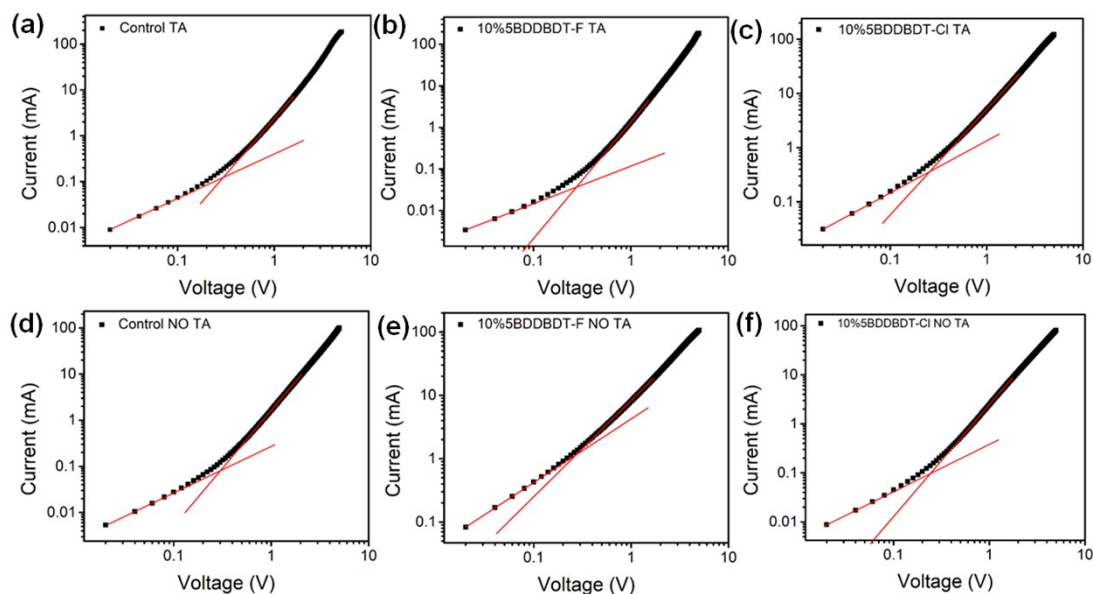


**Figure S7.**  $J$ - $V$  characteristics in the dark for electron-only devices base on control, 5BDDDBDT-F and 5BDDDBDT-CI with TA and without TA treatment.

**Table S4.** Hole and electron mobilities of the devices based on PM6:BTP-BO4Cl, PM6:5BDDDBDT-F:BTP-BO4Cl and PM6:5BDDDBDT-CI:BTP-BO4Cl blend films under optimal conditions

Active layer	Treatment	$\mu_h$ ( $\text{cm}^2 \text{V}^{-1} \text{s}^{-1}$ )	$\mu_e$ ( $\text{cm}^2 \text{V}^{-1} \text{s}^{-1}$ )	$\mu_h/\mu_e$
PM6:BTP-BO4Cl	TA	$1.02 \times 10^{-4}$	$1.83 \times 10^{-4}$	1.79
	NO TA	$1.35 \times 10^{-4}$	$1.35 \times 10^{-4}$	1
PM6:5BDDDBDT-F:BTP-BO4Cl	TA	$1.09 \times 10^{-4}$	$1.61 \times 10^{-4}$	1.48
	NO TA	$1.42 \times 10^{-4}$	$1.38 \times 10^{-4}$	0.97
PM6:5BDDDBDT-	TA	$1.26 \times 10^{-4}$	$2.0 \times 10^{-4}$	1.59

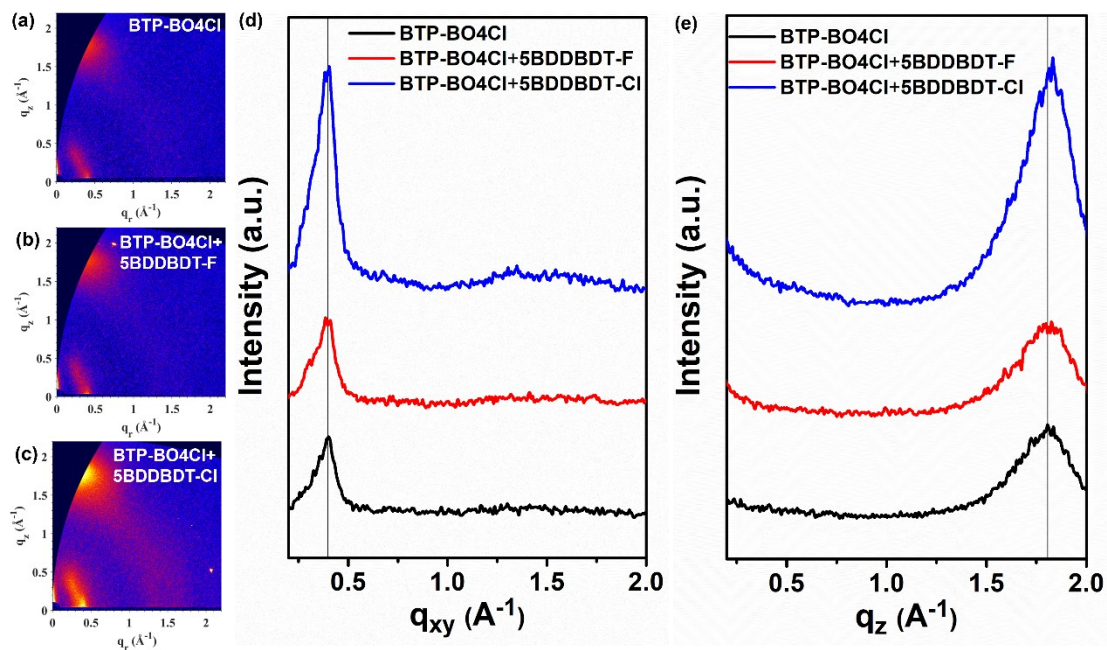


**Figure S8.** 2D-GIWAXS of BTP-BO4Cl neat films, BTP-BO4Cl:5BDDBDT-F blend films, and BTP-BO4Cl:5BDDBDT-Cl blend films.

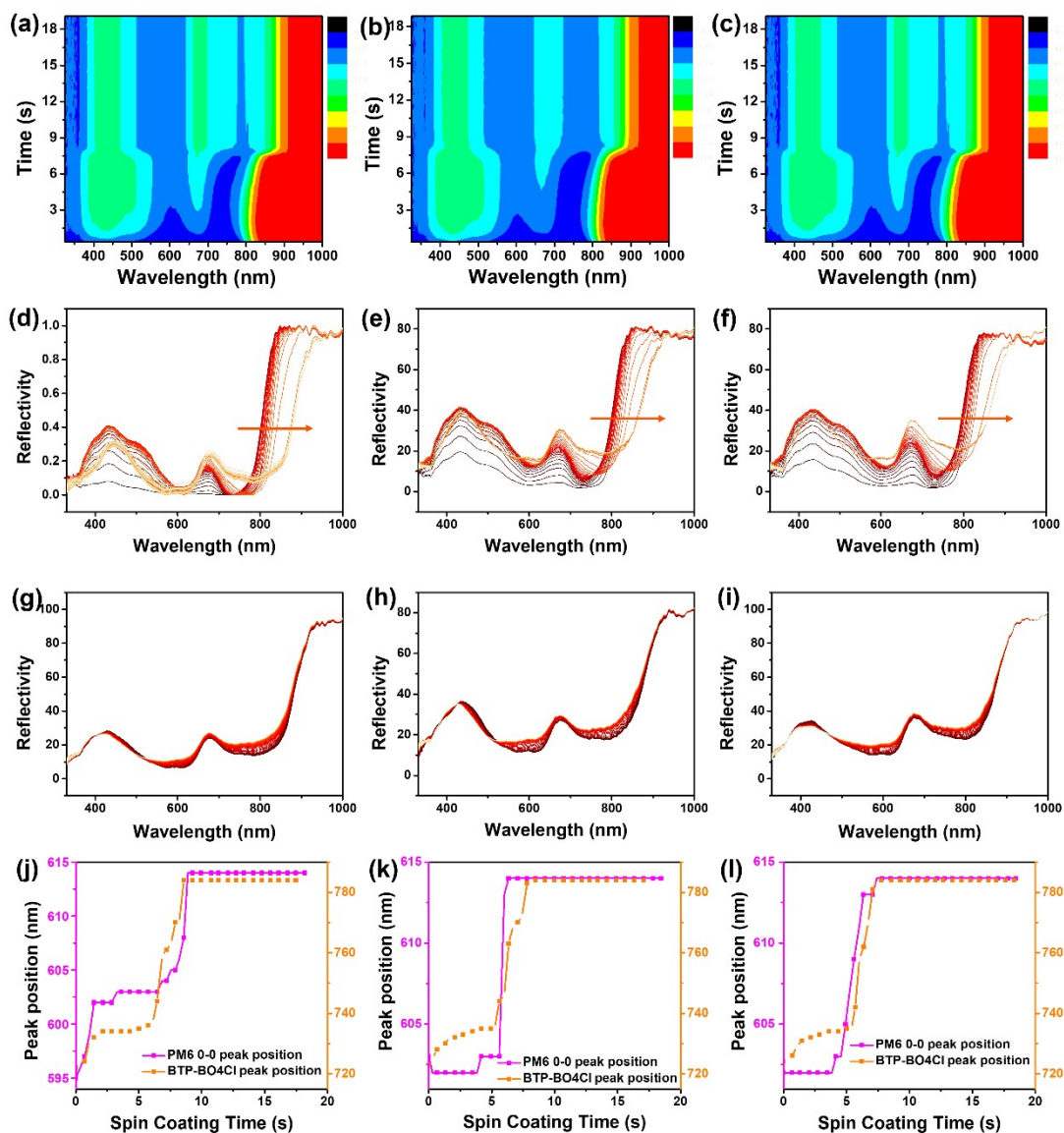


**Figure S9.** a-f) Time-dependent of situ UV-vis absorption spectra during spin coating processes without TA, g-i) Time-dependent of situ UV-vis absorption spectra during TA processes, j-l) Peak position of PM6 and BTP-BO4Cl during spin coating processes.

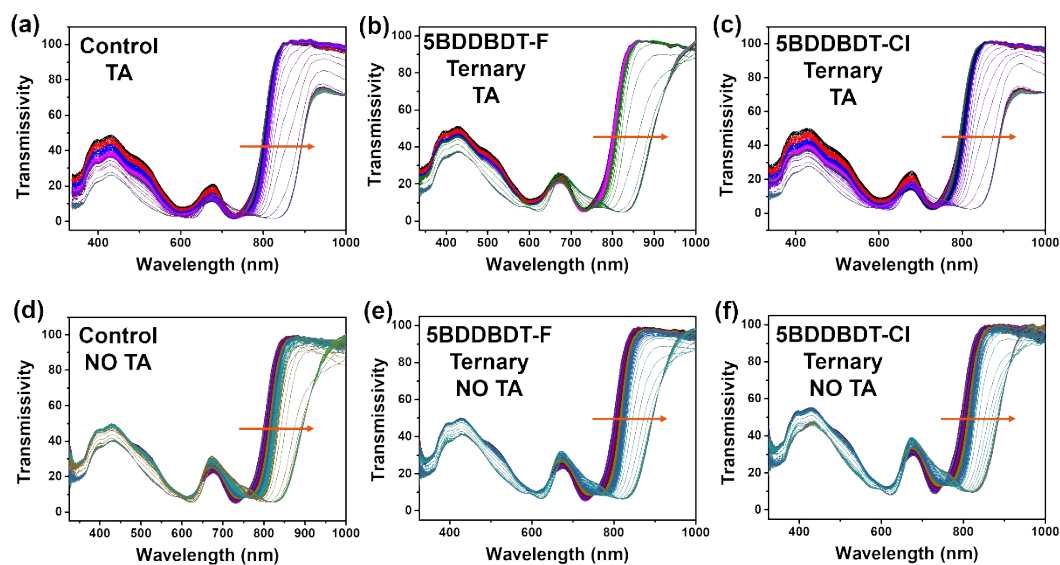


**Figure S10.** a-f) Time-dependent of situ UV-vis absorption spectra during blade coating processes.

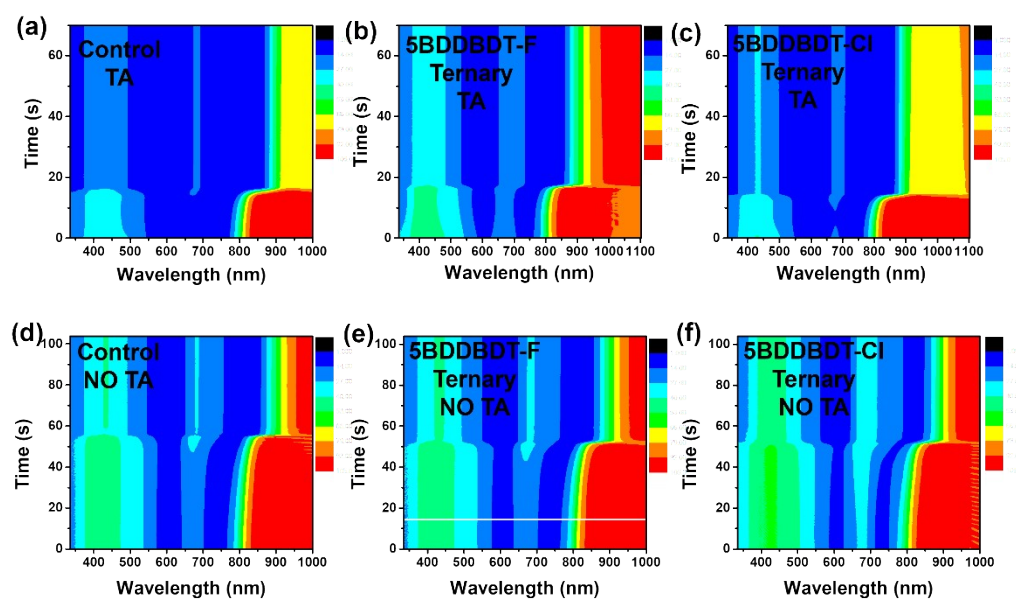


**Figure S11.** a-f) 2D Time-dependent of situ UV-vis absorption spectra during blade coating processes.

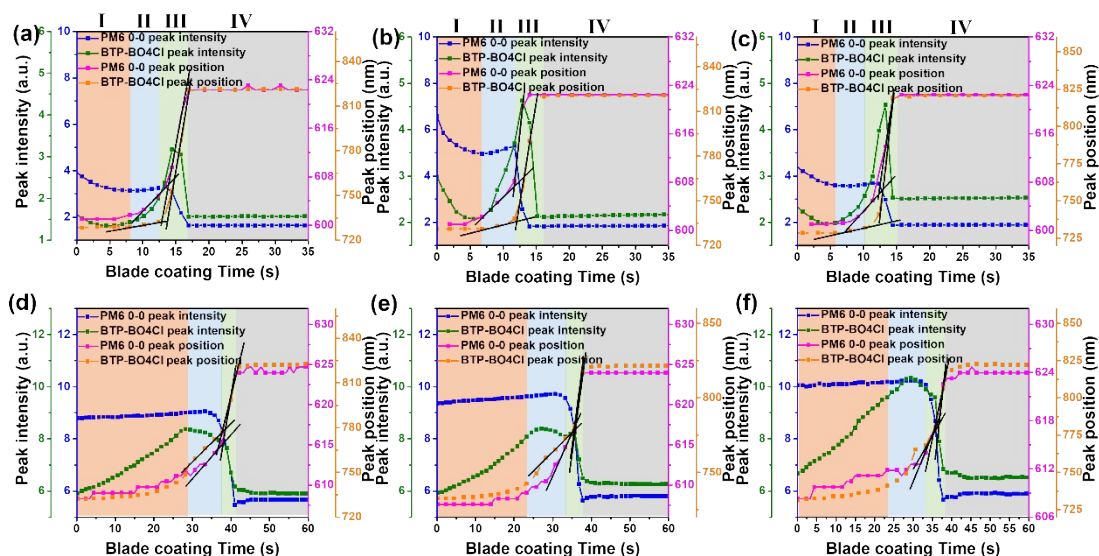


**Figure S12.** Time-dependent PM6 0–0 peak, BTP-BO4Cl peak and peak intensity evolution monitored by in situ UV-vis absorption spectra during blade coating processes with TA (a-c) and without TA (d-f).

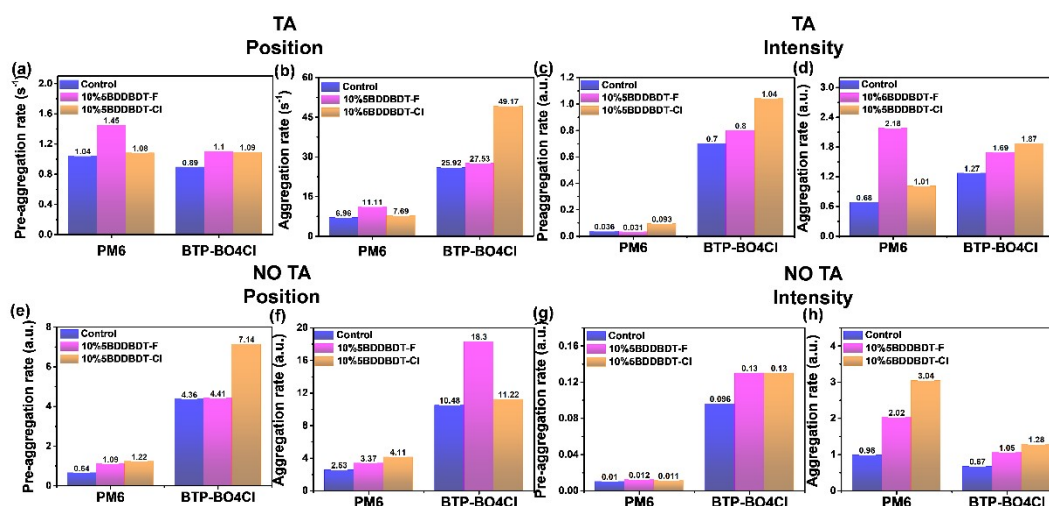


**Figure S13.** Pre-aggregation rates and Aggregation rates of donor and acceptor of the corresponding films during blade coating processes with TA (a-d) or without TA (e-f) according to changes in position and intensity.

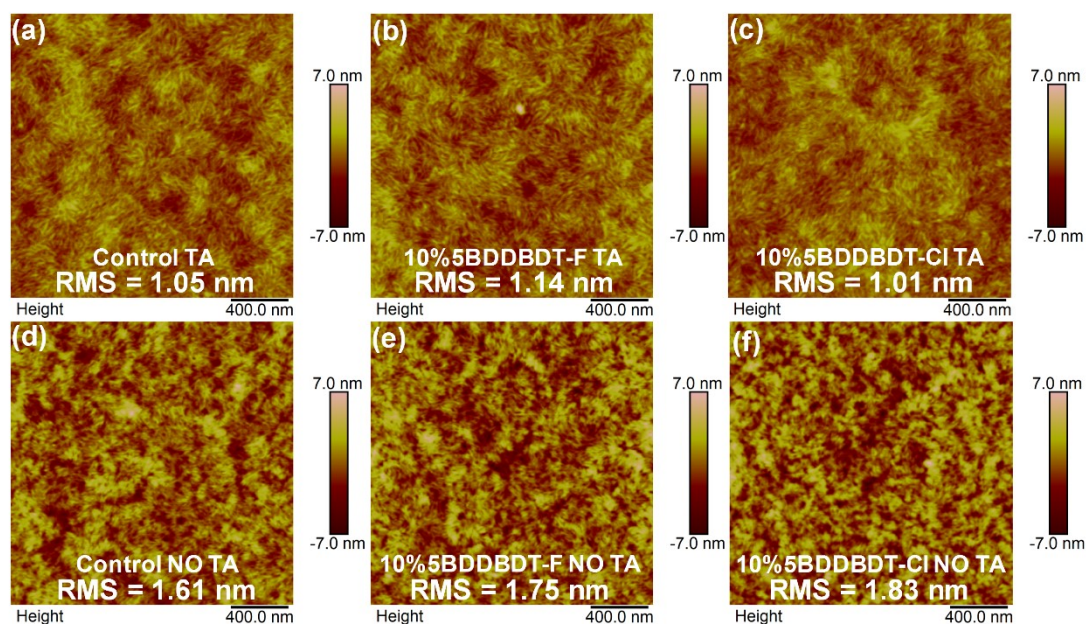


**Figure S14.** AFM height images of control, 10%5BDDBDT-F and 10%5BDDBDT-CI ternary blend films with a-c) TA and without d-f) TA.

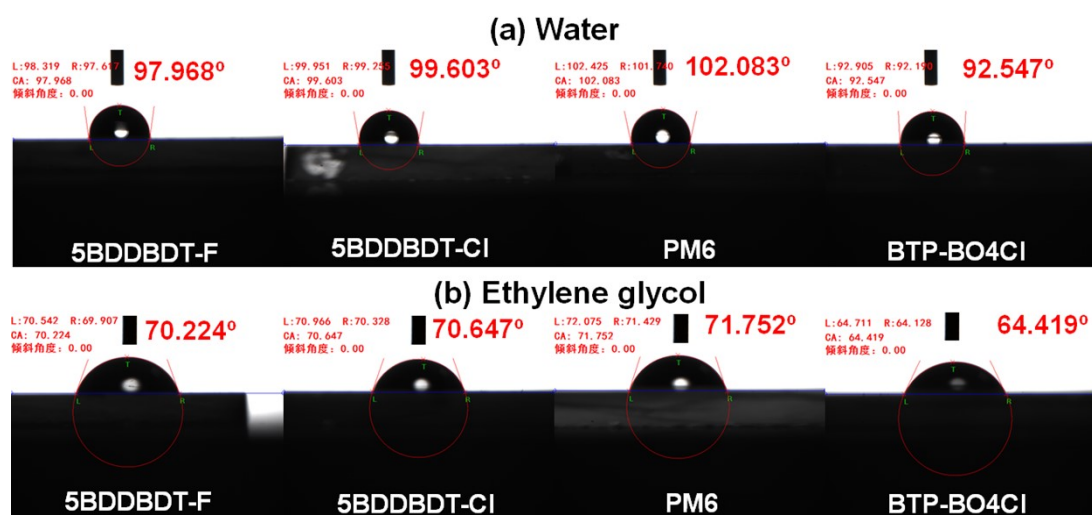


**Figure S15.** a, b) The contact angle images of pure films 5BDDBDT-F, 5BDDBDT-CI, PM6 and BTP-BO4Cl.

**Table S5.** Contact angle, surface tension and interfacial tension ( $\gamma$ ) of individual materials

Materials	WCA [°]	EgCA [°]	$\gamma^d$ [mN m <sup>-1</sup> ]	$\gamma^p$ [mN m <sup>-1</sup> ]	$\gamma$ [mN m <sup>-1</sup> ]	$\gamma^{\text{Donor-Acceptor}}$
5BDDBDT-F	97.968	70.224	26.222	1.087	27.308	0.382
5BDDBDT-CI	99.603	70.647	28.111	0.609	28.719	0.932
PM6	102.083	71.752	30.268	0.187	30.456	1.908
BTP-BO4Cl	92.547	64.419	26.832	2.202	29.033	--

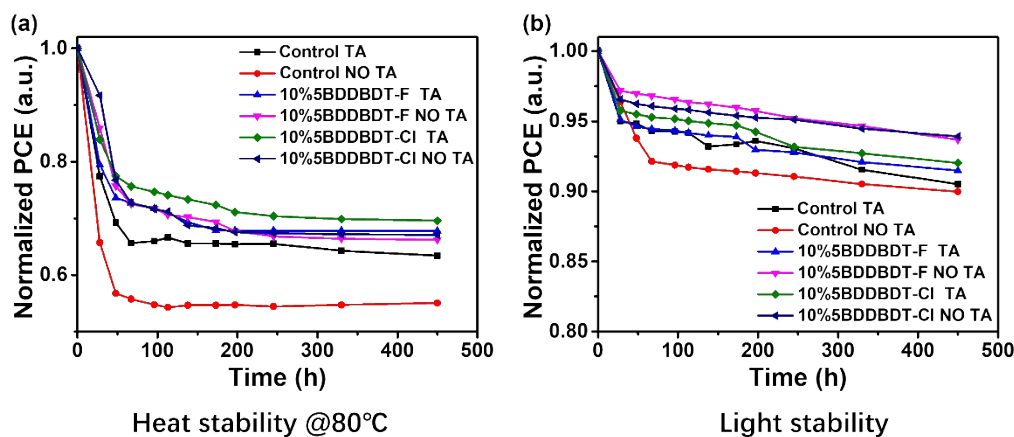


**Figure S16.** Evolution of PCEs of devices under 80 °C heating (a) and light (b).

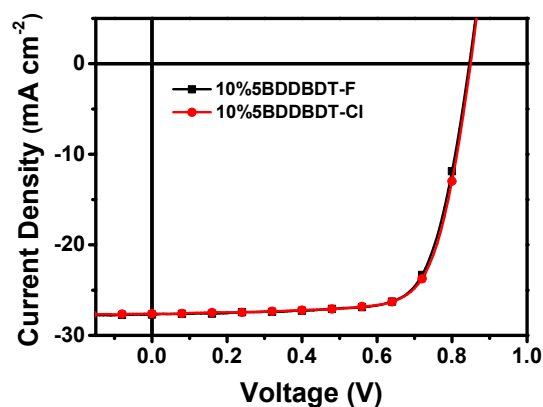
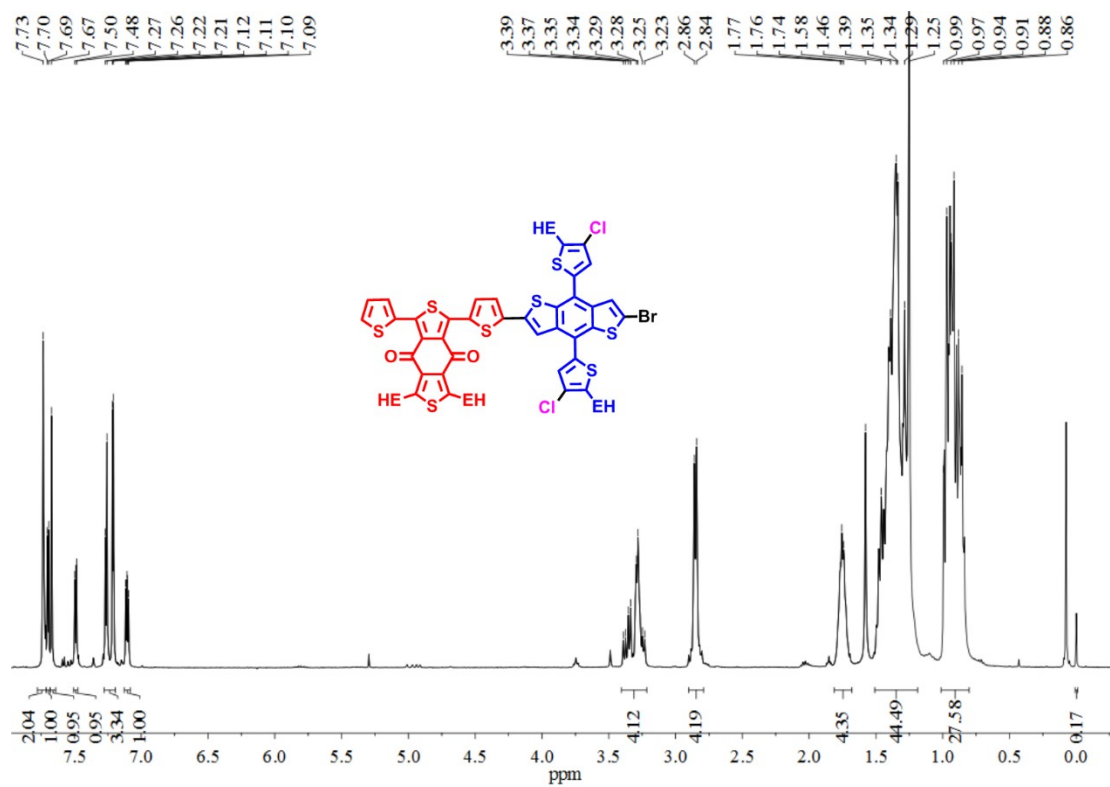
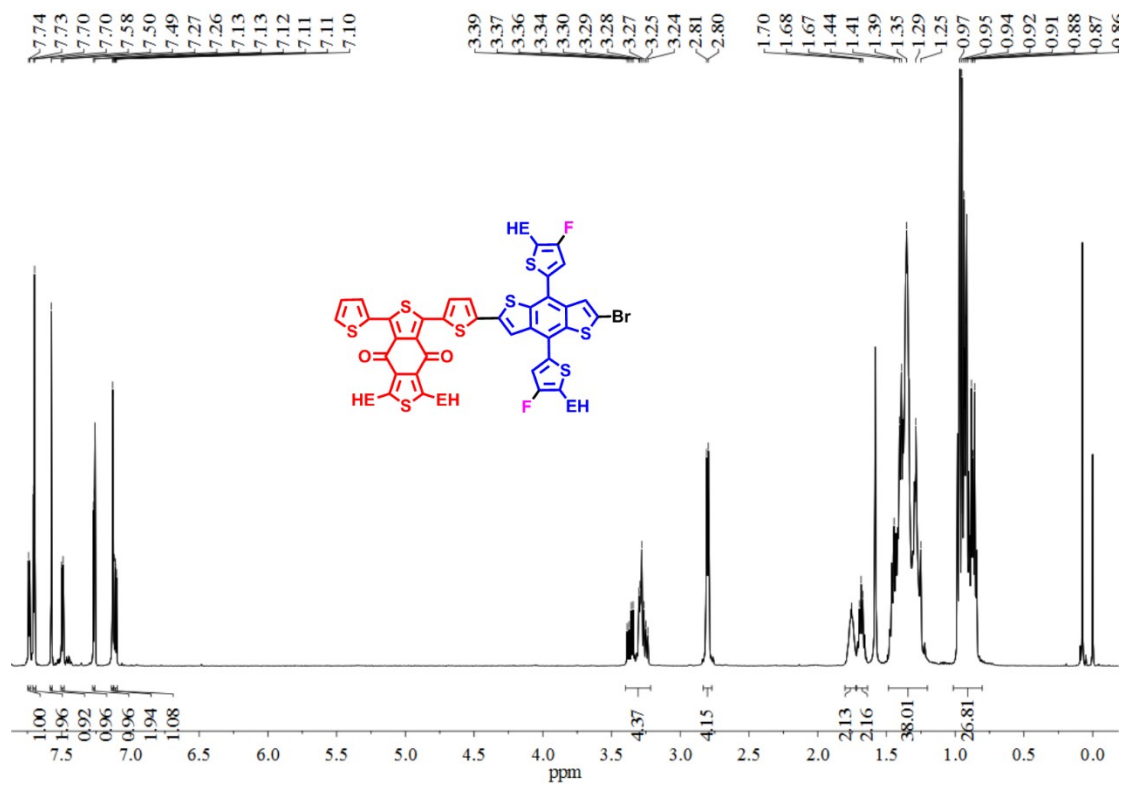


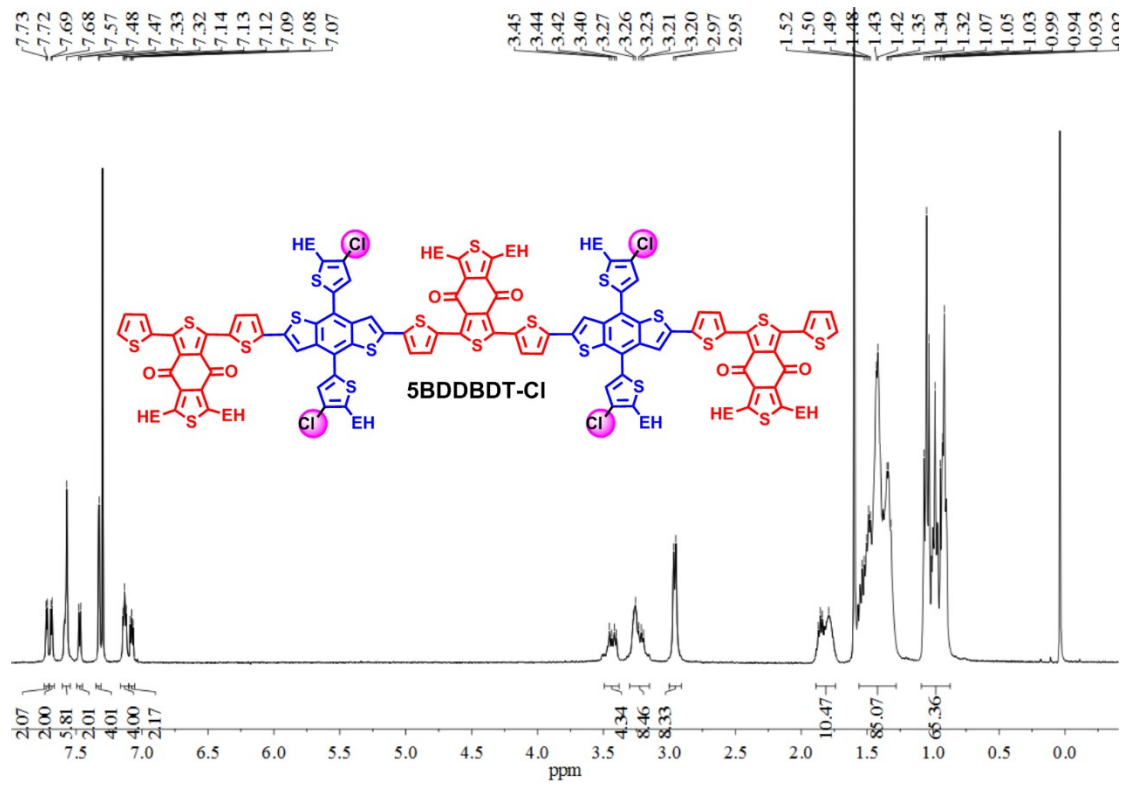
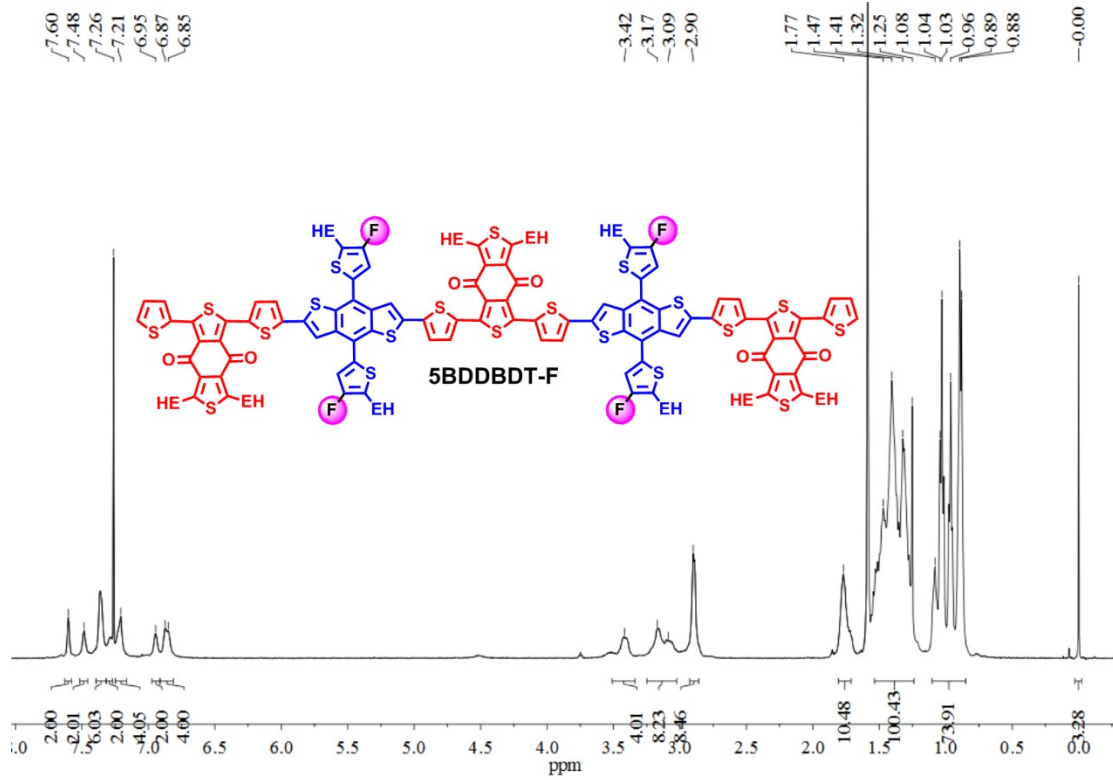
**Figure S17.** The  $J - V$  curves for 1 cm<sup>2</sup> ternary blade-coated devices based on PM6:oligomer:BTP-eC9 system without TA treatment were obtained under simulated AM 1.5 G irradiation at 100 mW cm<sup>-2</sup>, and these results were certified at Prof. Alex Jen's Group at the City University of Hong Kong.

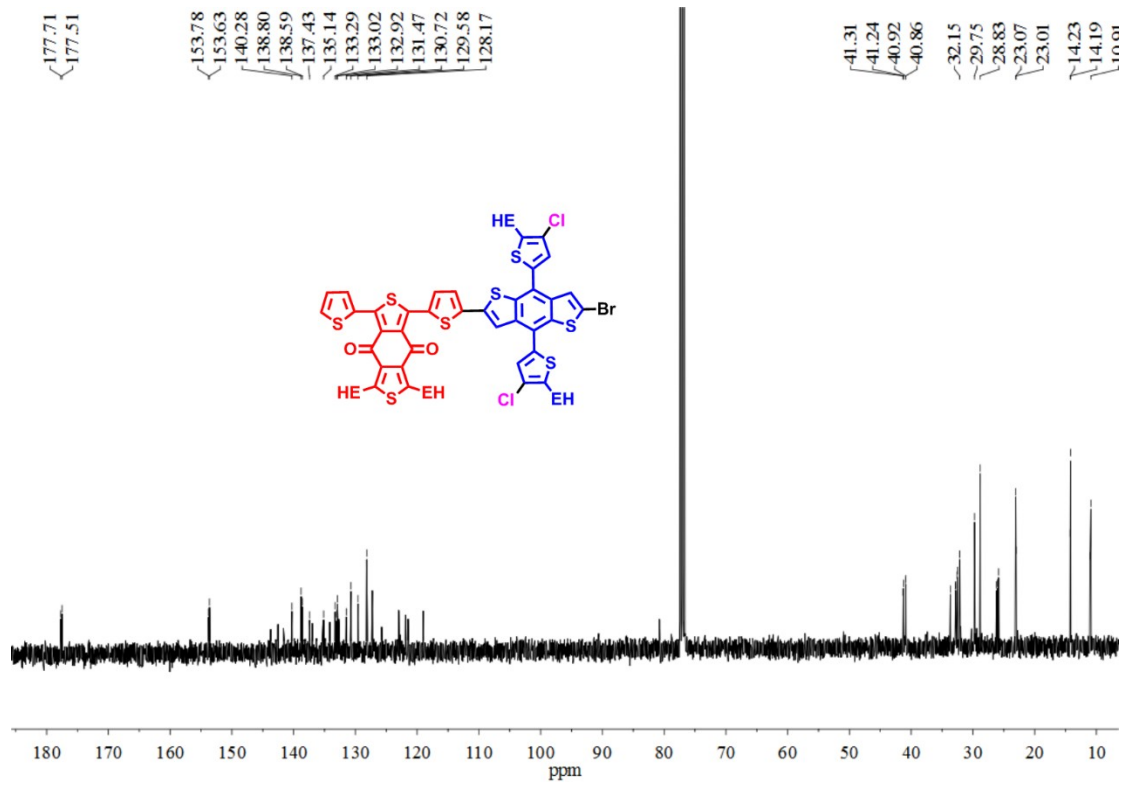
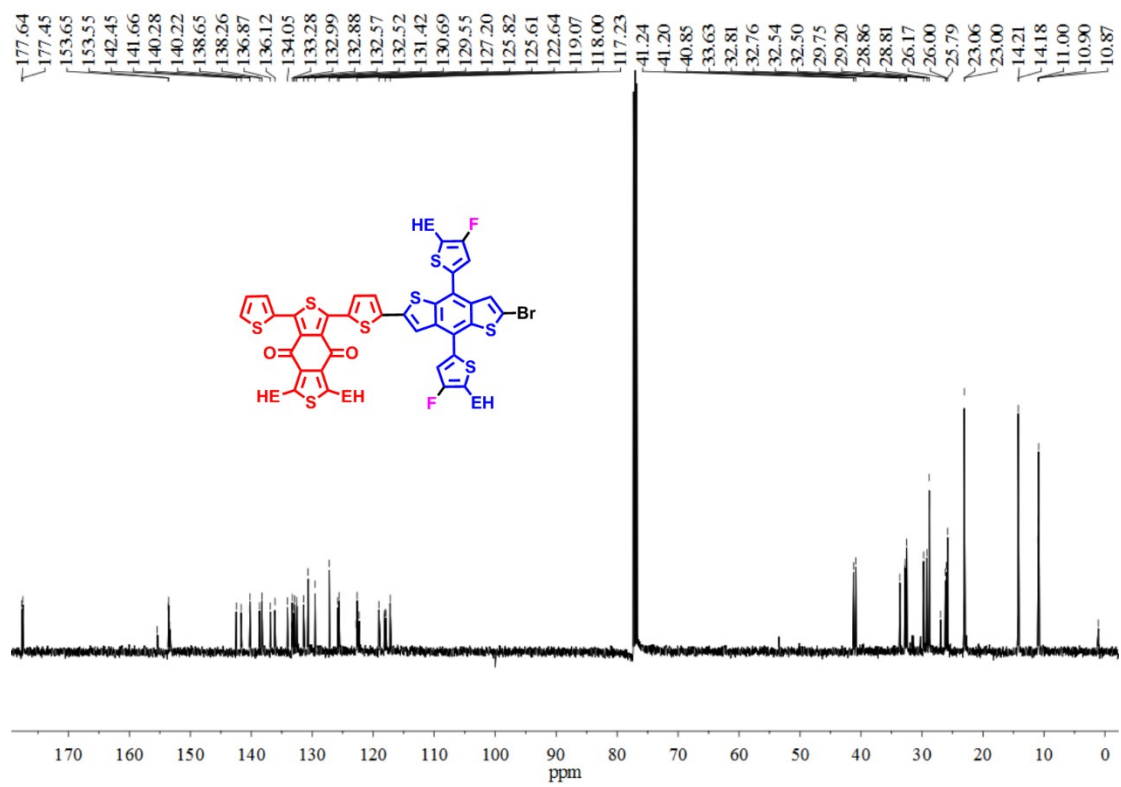
**Table S6.** The photovoltaic parameters for 1 cm<sup>2</sup> ternary blade-coated devices based on PM6:oligomer: BTP-eC9 system without TA treatment, which were certified at Prof. Alex Jen's Group at the City University of Hong Kong.

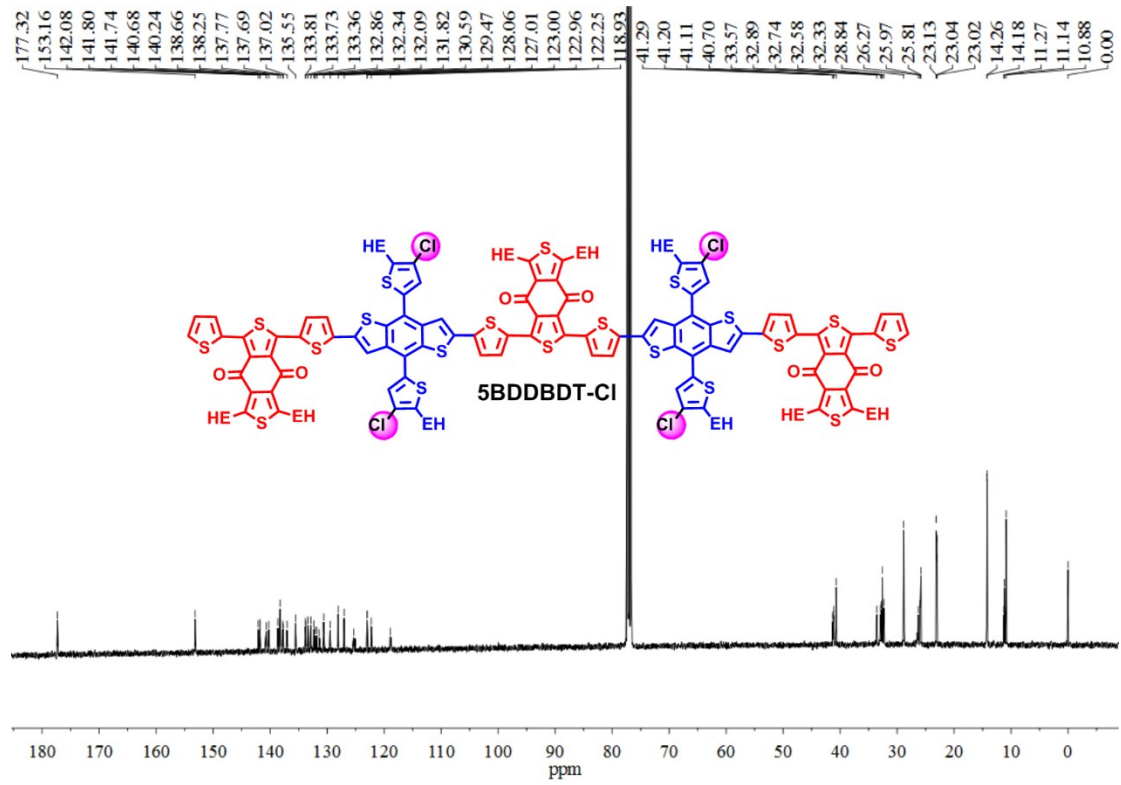
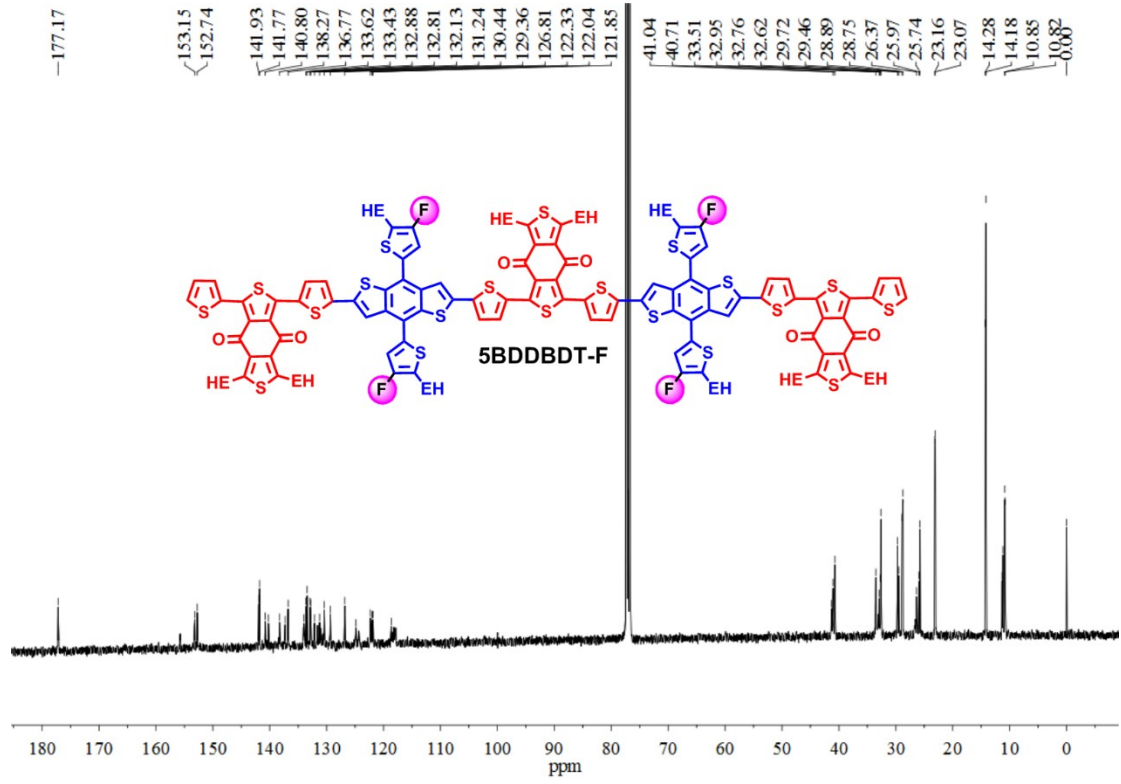
Third component	Area (cm <sup>2</sup> )	Coating method	Treatment	$V_{OC}$ (V)	$J_{sc}^a$ (mA cm <sup>-2</sup> )	FF (%)	$PCE_{max}^b$ (%)
10%5BDDBDT-F	1.003	Blade coating	NO TA	0.846	27.62	73.70	17.22
10%5BDDBDT-Cl	1.001	Blade coating	NO TA	0.850	27.57	74.13	17.37

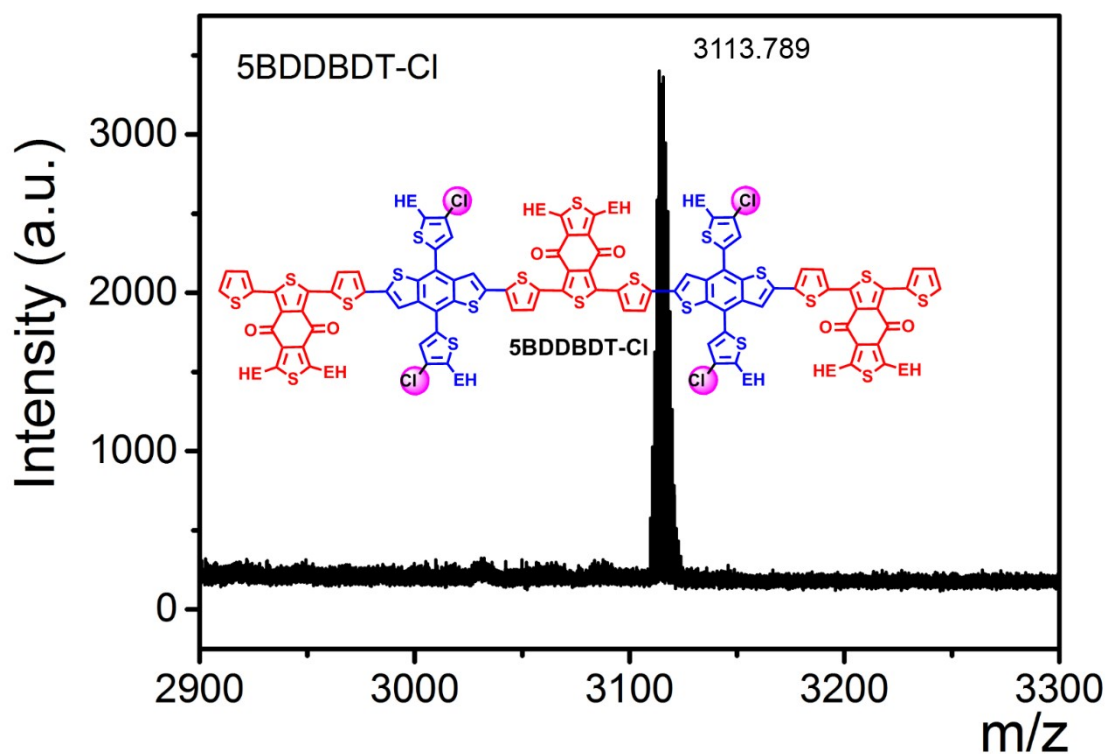
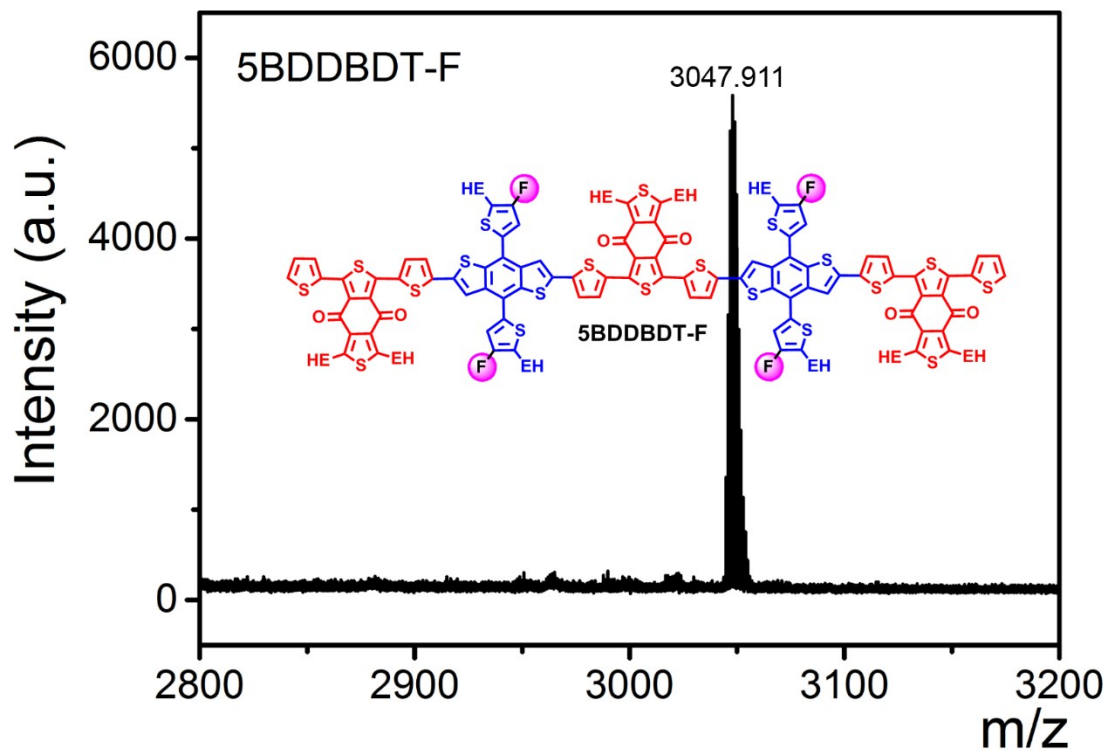
## 5. $^1\text{H-NMR}$ , $^{13}\text{C-NMR}$ and MALDI-TOF.











## References

- [1] J. Zhang, Y. Han, W. Zhang, J. Ge, L. Xie, Z. Xia, W. Song, D. Yang, X. Zhang, Z. Ge, *ACS Applied Materials & Interfaces* **2020**, *12*, 57271-57280.

- [2] H. Feng, X. Song, Z. Zhang, R. Geng, J. Yu, L. Yang, D. Baran, W. Tang, *Advanced Functional Materials* **2019**, *29*, 1903269.
- [3] L. Zhu, M. Zhang, G. Zhou, T. Hao, J. Xu, J. Wang, C. Qiu, N. Prine, J. Ali, W. Feng, X. Gu, Z. Ma, Z. Tang, H. Zhu, L. Ying, Y. Zhang, F. Liu, *Advanced Energy Materials* **2020**, *10*, 1904234.
- [4] C. Zhu, J. Yuan, F. Cai, L. Meng, H. Zhang, H. Chen, J. Li, B. Qiu, H. Peng, S. Chen, Y. Hu, C. Yang, F. Gao, Y. Zou, Y. Li, *Energy & Environmental Science* **2020**, *13*, 2459-2466.
- [5] F. Du, H. Wang, Z. Zhang, L. Yang, J. Cao, J. Yu, W. Tang, *Materials Horizons* **2021**, *8*, 1008-1016.
- [6] S. Huang, L. Duan, D. Zhang, *Journal of Materials Chemistry A* **2020**, *8*, 18792-18801.
- [7] J. Wan, R. Wen, Y. Xia, M. Dai, H. Huang, L. Xue, Z. Zhang, J. Fang, K. N. Hui, X. Fan, *Journal of Materials Chemistry A* **2021**, *9*, 5425-5433.
- [8] Z. Zhang, Y. Li, G. Cai, Y. Zhang, X. Lu, Y. Lin, *Journal of the American Chemical Society* **2020**, *142*, 18741-18745.
- [9] R. Ma, Y. Tao, Y. Chen, T. Liu, Z. Luo, Y. Guo, Y. Xiao, J. Fang, G. Zhang, X. Li, X. Guo, Y. Yi, M. Zhang, X. Lu, Y. Li, H. Yan, *Science China Chemistry* **2021**, *64*, 581-589.
- [10] X. Han, J. Zhu, Y. Xiao, H. Jiang, Z. Zhang, J. Wang, Z. Li, Y. Lin, X. Lu, X. Zhan, *Solar RRL* **2020**, *4*, 2000108.
- [11] X. Song, P. Sun, D. Sun, Y. Xu, Y. Liu, W. Zhu, *Nano Energy* **2022**, *91*, 106678.
- [12] H. Chen, R. Zhang, X. Chen, G. Zeng, L. Kobera, S. Abbrent, B. Zhang, W. Chen, G. Xu, J. Oh, S.-H. Kang, S. Chen, C. Yang, J. Brus, J. Hou, F. Gao, Y. Li, Y. Li, *Nature Energy* **2021**, *6*, 1045-1053.
- [13] S. Liu, J. Yuan, W. Deng, M. Luo, Y. Xie, Q. Liang, Y. Zou, Z. He, H. Wu, Y. Cao, *Nature Photonics* **2020**, *14*, 300-305.
- [14] L. Zhong, S. H. Kang, J. Oh, S. Jung, Y. Cho, G. Park, S. Lee, S. J. Yoon, H. Park, C. Yang, *Advanced Functional Materials* **2022**, *32*, 2201080.
- [15] S. Lee, G. Park, M. Jeong, B. Lee, S. Jeong, J. Park, Y. Cho, S. M. Noh, C. Yang,

- ACS Applied Materials & Interfaces* **2022**, *14*, 33614-33625.
- [16] Y. Han, W. Song, J. Zhang, L. Xie, J. Xiao, Y. Li, L. Cao, S. Song, E. Zhou, Z. Ge, *Journal of Materials Chemistry A* **2020**, *8*, 22155-22162.
- [17] W. Sun, H. Chen, B. Zhang, Q. Cheng, H. Yang, Z. Chen, G. Zeng, J. Ding, W. Chen, Y. Li, *Chinese Journal of Chemistry* **2022**, *40*, 2963-2972.
- [18] J. S. Park, C. Sun, Y. Han, G.-U. Kim, T. N.-L. Phan, Y.-H. Kim, B. J. Kim, *Advanced Energy and Sustainability Research* **2022**, *3*, 2200070.
- [19] S. Jeong, J. Park, Y. Ji, Y. Cho, B. Lee, M. Jeong, S. Jung, S. Yang, Y. Zhang, S.-J. Yoon, C. Yang, *Journal of Materials Chemistry A* **2023**, *11*, 4703-4716.
- [20] C.-P. Chen, C.-I. Liu, Y.-C. Peng, B.-H. Jiang, S.-J. Liu, C.-C. Yang, Y.-Y. Yu, *Materials Chemistry and Physics* **2022**, *285*, 126061.
- [21] Q. Fan, W. Su, M. Zhang, J. Wu, Y. Jiang, X. Guo, F. Liu, T. P. Russell, M. Zhang, Y. Li, *Solar RRL* **2019**, *3*, 1900169.
- [22] S. Dong, K. Zhang, T. Jia, W. Zhong, X. Wang, F. Huang, Y. Cao, *EcoMat* **2019**, *1*.
- [23] Q. Kang, L. Ye, B. Xu, C. An, S. J. Stuard, S. Zhang, H. Yao, H. Ade, J. Hou, *Joule* **2019**, *3*, 227-239.
- [24] Z. Xing, X. Meng, R. Sun, T. Hu, Z. Huang, J. Min, X. Hu, Y. Chen, *Advanced Functional Materials* **2020**, *30*, 2000417.
- [25] Q. Kang, Z. Zheng, Y. Zu, Q. Liao, P. Bi, S. Zhang, Y. Yang, B. Xu, J. Hou, *Joule* **2021**, *5*, 646-658.
- [26] Y. Li, H. Liu, J. Wu, H. Tang, H. Wang, Q. Yang, Y. Fu, Z. Xie, *ACS Applied Materials & Interfaces* **2021**, *13*, 10239-10248.
- [27] J. Zhang, L. Zhang, X. Wang, Z. Xie, L. Hu, H. Mao, G. Xu, L. Tan, Y. Chen, *Advanced Energy Materials* **2022**, *12*, 2200165.
- [28] W. Zhao, S. Zhang, Y. Zhang, S. Li, X. Liu, C. He, Z. Zheng, J. Hou, *Advanced Materials* **2018**, *30*, 1704837.
- [29] S. Dong, K. Zhang, B. Xie, J. Xiao, H.-L. Yip, H. Yan, F. Huang, Y. Cao, *Advanced Energy Materials* **2019**, *9*, 1802832.
- [30] Y. Cui, H. Yao, L. Hong, T. Zhang, Y. Xu, K. Xian, B. Gao, J. Qin, J. Zhang, Z.

- Wei, J. Hou, *Advanced Materials* **2019**, *31*, 1808356.
- [31] D. Chen, S. Liu, B. Huang, J. Oh, F. Wu, J. Liu, C. Yang, L. Chen, Y. Chen, *Small* **2022**, *18*, 2200734.
- [32] L. Hong, H. Yao, Z. Wu, Y. Cui, T. Zhang, Y. Xu, R. Yu, Q. Liao, B. Gao, K. Xian, H. Y. Woo, Z. Ge, J. Hou, *Advanced Materials* **2019**, *31*, 1903441.
- [33] L. Zhang, S. Yang, B. Ning, F. Yang, W. Deng, Z. Xing, Z. Bi, K. Zhou, Y. Zhang, X. Hu, B. Yang, J. Yang, Y. Zou, W. Ma, Y. Yuan, *Solar RRL* **2021**, *6*, 2100838.
- [34] Q. Kang, Y. Zu, Q. Liao, Z. Zheng, H. Yao, S. Zhang, C. He, B. Xu, J. Hou, *Journal of Materials Chemistry A* **2020**, *8*, 5580-5586.
- [35] X. Song, Y. Song, H. Xu, S. Gao, Y. Wang, J. Li, J. Hai, W. Liu, W. Zhu, *Advanced Energy Materials* **2022**, *13*, 2203009.
- [36] G. Du, Z. Wang, T. Zhai, Y. Li, K. Chang, B. Yu, X. Zhao, W. Deng, *ACS Applied Materials & Interfaces* **2022**, *14*, 13572-13583.
- [37] H. Yu, M. Pan, R. Sun, I. Agunawela, J. Zhang, Y. Li, Z. Qi, H. Han, X. Zou, W. Zhou, S. Chen, J. Lai, S. Luo, Z. Luo, D. Zhao, X. Lu, H. Ade, F. Huang, J. Min, H. Yan, *Angewandte Chemie International Edition* **2021**, *60*, 10137-10146.
- [38] S. Yoon, S. Park, S. H. Park, S. Nah, S. Lee, J.-W. Lee, H. Ahn, H. Yu, E.-Y. Shin, B. J. Kim, B. K. Min, J. H. Noh, H. J. Son, *Joule* **2022**, *6*, 2406-2422.
- [39] G. Zeng, W. Chen, X. Chen, Y. Hu, Y. Chen, B. Zhang, H. Chen, W. Sun, Y. Shen, Y. Li, F. Yan, Y. Li, *Journal of the American Chemical Society* **2022**, *144*, 8658-8668.
- [40] J. Wang, M. Zhang, J. Lin, Z. Zheng, L. Zhu, P. Bi, H. Liang, X. Guo, J. Wu, Y. Wang, L. Yu, J. Li, J. Lv, X. Liu, F. Liu, J. Hou, Y. Li, *Energy & Environmental Science* **2022**, *15*, 1585-1593.
- [41] Y. Yang, J. Wang, Y. Zu, Q. Liao, S. Zhang, Z. Zheng, B. Xu, J. Hou, *Joule* **2023**, *7*, 545-557.